

Functional Differences in Ionic Regulation between Alternatively Spliced Isoforms of the Na⁺-Ca²⁺ Exchanger from *Drosophila melanogaster*

ALEXANDER OMELCHENKO,* CHRISTOPHER DYCK,* MARK HNATOWICH,* JOHN BUCHKO,*
DEBORA A. NICOLL,^{†§} KENNETH D. PHILIPSON,^{†§} and LARRY V. HRYSHKO*

From the *Institute of Cardiovascular Sciences, St. Boniface General Hospital Research Centre, Winnipeg, Manitoba, Canada R2H 2A6; and [†]Department of Physiology, and [§]Department of Medicine and the Cardiovascular Research Laboratories, University of California, Los Angeles, Los Angeles, California 90025-1760

ABSTRACT Ion transport and regulation were studied in two, alternatively spliced isoforms of the Na⁺-Ca²⁺ exchanger from *Drosophila melanogaster*. These exchangers, designated CALX1.1 and CALX1.2, differ by five amino acids in a region where alternative splicing also occurs in the mammalian Na⁺-Ca²⁺ exchanger, NCX1. The CALX isoforms were expressed in *Xenopus laevis* oocytes and characterized electrophysiologically using the giant, excised patch clamp technique. Outward Na⁺-Ca²⁺ exchange currents, where pipette Ca²⁺_o exchanges for bath Na⁺_i, were examined in all cases. Although the isoforms exhibited similar transport properties with respect to their Na⁺_i affinities and current-voltage relationships, significant differences were observed in their Na⁺_i- and Ca²⁺_i-dependent regulatory properties. Both isoforms underwent Na⁺_i-dependent inactivation, apparent as a time-dependent decrease in outward exchange current upon Na⁺_i application. We observed a two- to threefold difference in recovery rates from this inactive state and the extent of Na⁺_i-dependent inactivation was approximately twofold greater for CALX1.2 as compared with CALX1.1. Both isoforms showed regulation of Na⁺-Ca²⁺ exchange activity by Ca²⁺_i, but their responses to regulatory Ca²⁺_i differed markedly. For both isoforms, the application of cytoplasmic Ca²⁺_i led to a decrease in outward exchange currents. This negative regulation by Ca²⁺_i is unique to Na⁺-Ca²⁺ exchangers from *Drosophila*, and contrasts to the positive regulation produced by cytoplasmic Ca²⁺ for all other characterized Na⁺-Ca²⁺ exchangers. For CALX1.1, Ca²⁺_i inhibited peak and steady state currents almost equally, with the extent of inhibition being ≈80%. In comparison, the effects of regulatory Ca²⁺_i occurred with much higher affinity for CALX1.2, but the extent of these effects was greatly reduced (≈20–40% inhibition). For both exchangers, the effects of regulatory Ca²⁺_i occurred by a direct mechanism and indirectly through effects on Na⁺_i-induced inactivation. Our results show that regulatory Ca²⁺_i decreases Na⁺_i-induced inactivation of CALX1.2, whereas it stabilizes the Na⁺_i-induced inactive state of CALX1.1. These effects of Ca²⁺_i produce striking differences in regulation between CALX isoforms. Our findings indicate that alternative splicing may play a significant role in tailoring the regulatory profile of CALX isoforms and, possibly, other Na⁺-Ca²⁺ exchange proteins.

KEY WORDS: *Drosophila melanogaster* • sodium-calcium exchange • regulation • alternative splicing

INTRODUCTION

Sodium-calcium exchange plays a major role in Ca²⁺ homeostasis in a wide variety of tissues (Lederer et al., 1996). In cardiac muscle, for example, the Na⁺-Ca²⁺ exchanger is the primary mechanism for transsarcolemmal Ca²⁺ efflux enabling cardiac relaxation (Bers, 1991). Similarly, in neuronal tissue, the exchanger may play an important role in Ca²⁺ efflux and, thus, excitation-secretion coupling (Blaustein et al., 1996). Calcium removal is accomplished by coupling the energy in the Na⁺ electrochemical gradient to the uphill movement of Ca²⁺. Moreover, as a reversible transporter, the Na⁺-Ca²⁺ exchanger may also mediate Ca²⁺ entry, a role

recently postulated for excitation of cardiac muscle (Leblanc and Hume, 1990; Levi et al., 1994).

Two forms of ionic regulation have been characterized extensively for the cardiac Na⁺-Ca²⁺ exchanger, NCX1, using the giant, excised patch clamp technique (Hilgemann et al., 1992a, 1992b). These regulatory processes are controlled by Na⁺ and Ca²⁺ and are most readily observed for outward Na⁺-Ca²⁺ exchange currents, where extracellular Ca²⁺ exchanges for intracellular Na⁺. Upon application of Na⁺_i to evoke an outward exchange current, the current peaks and then decays to lower, steady state levels (Hilgemann, 1990). The extent and rate of current inactivation depends upon the concentration of applied Na⁺_i, a process referred to as Na⁺_i-induced (I₁)¹ inactivation (Hilgemann et al., 1992a). Calcium-induced (I₂) regulation describes the stimulatory influence of cytoplasmic Ca²⁺

Address correspondence to Larry V. Hryshko, Institute of Cardiovascular Sciences, St. Boniface General Hospital Research Centre, 351 Tache Avenue, Winnipeg, Manitoba, Canada R2H 2A6. Fax: 204-233-6723; E-mail: lhryshko@sbr.c.umanitoba.ca

¹Abbreviations used in this paper: I₁, Na⁺_i-induced; I₂, Ca²⁺_i-induced.

on outward exchange currents, evident at submicromolar Ca^{2+}_i concentrations (Hilgemann et al., 1992b). Outward exchange currents can be nearly eliminated in the absence of regulatory Ca^{2+}_i , despite approaching infinite electrochemical gradients favoring exchange (Hilgemann, 1990). Interactions are observed between Na^+_{i-} and Ca^{2+}_{i-} -mediated regulatory mechanisms. Most prominent is the observation that increasing regulatory Ca^{2+}_i can eliminate the Na^+_{i-} -induced inactivation in NCX1 (Hilgemann et al., 1992b). Mutations targeting Ca^{2+}_{i-} -dependent regulation also influence the behavior of I_1 inactivation and vice versa (Matsuoka et al., 1993, 1995, 1997). The physiological significance of these ionic regulatory mechanisms remains largely unknown.

The *Drosophila* $\text{Na}^+/\text{Ca}^{2+}$ exchanger, CALX1.1, also exhibits the two forms of ionic regulation observed with NCX1 (Hryshko et al., 1996). However, it is unique among members of this multigene family of transporters in that it is inhibited by cytoplasmic Ca^{2+} . All other characterized $\text{Na}^+/\text{Ca}^{2+}$ exchangers are stimulated by Ca^{2+}_i .

Sodium-calcium exchange activity is mediated by a single, integral membrane protein modeled to contain 11 transmembrane-spanning segments. Approximately one half of the protein mass resides in a large, intracellular loop located between transmembrane segments five and six (Nicoll et al., 1990; Hryshko and Philipson, 1997). Structure-function studies of NCX1 have identified discrete regions within this loop with important roles in the regulation of $\text{Na}^+/\text{Ca}^{2+}$ exchange activity (Matsuoka et al., 1993, 1995, 1997). For example, the XIP region near the NH_2 terminus of the intracellular loop is involved in Na^+_{i-} -induced regulation of exchange activity. Mutations within this 20 amino acid region can accelerate or eliminate the I_1 inactivation process (Matsuoka et al., 1997). Similarly, the regulatory Ca^{2+}_i binding site has been localized to a large central portion of the loop where two clusters of acidic amino acids are prominent (Levitsky et al., 1994). Mutation of residues within these clusters leads to substantial reductions in the affinity for regulatory Ca^{2+}_i (Matsuoka et al., 1995).

Recent studies have identified unique gene products and alternatively spliced isoforms of $\text{Na}^+/\text{Ca}^{2+}$ exchangers in a wide array of tissues. (Lee et al., 1994; Kofuji et al., 1994; Lederer et al., 1996; Quednau et al., 1997; Barnes et al., 1997). At least two splice variants of the $\text{Na}^+/\text{Ca}^{2+}$ exchanger from *Drosophila melanogaster* have been identified (Ruknudin et al., 1997; Schwarz and Benzer, 1997). The existence of tissue-specific, alternatively spliced isoforms, as well as unique gene products, suggests that exchange function might be specifically tailored to the Ca^{2+} homeostasis requirements of individual tissues. However, experimental evidence supporting this notion is lacking. In this study, we charac-

terized the ionic regulatory properties of two splice variants from *Drosophila* using the giant, excised patch clamp technique and show, for the first time, that alternative splicing produces substantial differences in the characteristics of Na^+_{i-} and Ca^{2+}_{i-} -mediated regulation.

METHODS

Preparation of Xenopus laevis Oocytes

Xenopus laevis were anaesthetized in 250 mg/liter ethyl *p*-aminobenzoate (Sigma Chemical Co., St. Louis, MO) in deionized ice water for 30 min, the oocytes were then removed and washed in solution A containing (mM): 88 NaCl, 15 HEPES, 2.4 NaHCO_3 , 1.0 KCl, 0.82 MgSO_4 , pH 7.6. The follicles were teased apart, the oocytes (≈ 5 ml) transferred to 5 ml solution A containing 80 mg collagenase (Type II; Worthington Biochemical Corp., Freehold, NJ) and incubated for 40–45 min at room temperature with gentle agitation. The oocytes were washed free of collagenase in solution B (solution A plus 0.41 mM CaCl_2 and 0.3 mM $\text{Ca}(\text{NO}_3)_2$ containing 1 mg/ml BSA) (Fraction V; Sigma Chemical Co.), transferred to 5 ml of 100 mM K_2HPO_4 containing 1 mg/ml BSA and incubated for 11–12 min at room temperature with gentle agitation. After several washes in solution B plus BSA, defolliculated stage V and VI oocytes were selected and incubated at 16°C overnight in solution B.

Construction of Calx1.2

A λ phage partial clone containing the *Calx1.2* alternative exon was kindly provided by Dr. E. Schwarz (Columbia University, New York). DNA was PCR amplified from the phage using as primers GGTGATCGACGATGACGTATTTG (forward-1) and TCGCTT-TTGCCACCAGCTTG (reverse-1). The PCR product was subcloned into the pCR2.1 vector (Invitrogen Corp., San Diego, CA) and sequenced. One clone, I, contained the *Calx1.2* alternative exon encoding for the sequence STHYP. There were two additional base changes in the part of the PCR product that was used to construct the full length *Calx1.2*. Neither change (C to T at position 1990 or A to G at position 2083) altered the predicted translation product, but the second change deleted a BglIII restriction enzyme site. The BglIII restriction site was reintroduced in a second round of PCR using clone I as template and forward-1 primer with reverse-2 primer (GGTCAGATCTTGAACGGG). The resulting PCR product was subcloned into pCR2.1 and sequenced. The isolated clone, 2f, contained a BglIII site and no additional mutations. The full length *Calx1.2* was constructed by subcloning the EagI-BglIII fragment from 2f into the *Calx1.1* full length clone. The resulting clone contains only the alternative exon encoding STHYP and no other amino acid changes relative to CALX1.1.

Synthesis of CALX1.1 and CALX1.2 cRNAs

Complementary DNAs encoding CALX1.1 (previously referred to as Calx; Hryshko et al., 1996) and CALX1.2 were inserted into pBluescript II SK(+) (Stratagene Inc., La Jolla, CA), linearized with NotI (New England Biolabs Inc., Beverly, MA), and cRNA was synthesized using T7 mMessage mMachine in vitro transcription kits (Ambion Inc., Austin, TX), according to the manufacturer's instructions. After injection with ≈ 5 ng of cRNA encoding CALX1.1 or CALX1.2, oocytes were maintained at 16°C. Electrophysiological measurements were typically obtained from day 4 to 6 postinjection.

Measurement of Na⁺-Ca²⁺ Exchange Activity

Outward Na⁺-Ca²⁺ exchange currents were obtained using the giant, excised membrane patch technique, as described (Hilgemann, 1990; Hryshko et al., 1996; Trac et al., 1997). Borosilicate glass pipettes were pulled and polished to a final inner diameter of ≈20–30 μm and coated with a Parafilm™ (American National Can, Greenwich, CT):mineral oil mixture to enhance patch stability and reduce electrical noise. After removal of the vitellin layer by dissection, oocytes were placed in a solution containing (mM): 100 KOH, 100 MES, 20 HEPES, 5 EGTA, 5 MgCl₂, pH 7.0 at 30°C with MES (morpholine ethanesulfonic acid), and GΩ seals formed via gentle suction. Membrane patches (inside-out configuration) were excised by progressive movements of the pipette tip. Rapid (i.e., ≈0.2 s) bath solution (i.e., intracellular) changes were accomplished using a custom-built, computer-controlled, 20-channel solution switcher. Hardware and software (Axopatch 200a and Axotape, respectively; Axon Instruments, Foster City, CA) were used for data acquisition and analysis. Pipette (i.e., extracellular) solutions contained (mM): 100 NMG (*N*-methyl-D-glucamine)-MES, 30 HEPES, 30 TEA (tetraethyl ammonium)-OH, 16 sulfamic acid, 8 CaCO₃, 6 KOH, 0.25 ouabain, 0.1 niflumic acid, 0.1 flufenamic acid, pH 7.0 at 30°C with MES. Outward Na⁺-Ca²⁺ exchange currents were elicited by switching from Li⁺- to Na⁺-based bath solutions containing (mM): 100 [Na⁺ + Li⁺]-aspartate, 20 MOPS, 20 TEA-OH, 20 CsOH, 10 EGTA, 0–2.3 CaCO₃, 1.0–1.5 Mg(OH)₂, pH 7.0 at 30°C with MES or LiOH. Magnesium and Ca²⁺ were adjusted to yield free concentrations of 1.0 mM and 0–30 μM, respectively, using MAXC software (Bers et al., 1994). All experiments were conducted at 30 ± 1°C. All data reported are mean ± SEM unless indicated otherwise.

RESULTS

We characterized the transport and regulatory properties of two *Drosophila* Na⁺-Ca²⁺ exchanger isoforms, CALX1.1 and CALX1.2. Putative regions of functional importance for ionic regulation (Philipson et al., 1996), analogous to those identified in NCX1, are shown in Fig. 1. The location and amino acid sequence of the alternatively spliced region for the CALX isoforms is shown. The amino acid sequences (confirmed by dideoxy sequencing) conform to those reported by Schwarz and Benzer (1997) and differ from those reported by Ruknudin et al. (1997). Specifically, Schwarz and Benzer (1997) report that the amino acid sequences of the alternative splice variants are DELAA and STHYP for CALX1.1 and CALX1.2, respectively, whereas Ruknudin et al. (1997) found that the alternative splice variants encode for the amino acid sequences DGLAA and STHYR, respectively. It is not clear whether the reported differences are due to the presence of additional splice variants or to strain differences, although the latter seems more likely.

Na⁺ Dependence of Na⁺-Ca²⁺ Exchange

We examined the Na⁺ dependence of outward Na⁺-Ca²⁺ exchange currents in excised membrane patches from oocytes expressing CALX1.1 and CALX1.2. Fig. 2 shows current traces from single patches for each iso-

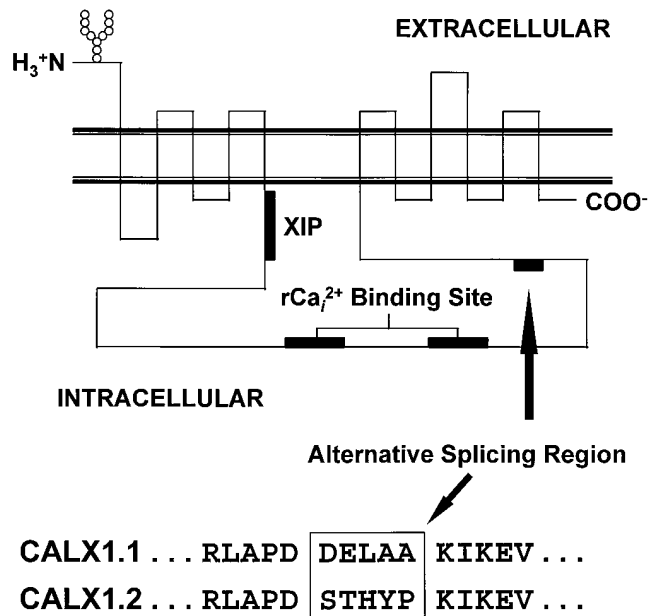


FIGURE 1. The putative topological organization of Na⁺-Ca²⁺ exchangers. Relative positions of the NH₃⁺ and COOH termini, N-linked glycosylation site, transmembrane-spanning domains, XIP region, regulatory Ca²⁺_i binding site, and location of the alternative splicing region are shown. The five amino acids that differ between CALX1.1 and CALX1.2 (verified by dideoxy sequencing) are shown boxed below using single-letter amino acid code.

form in which currents were elicited by the application of various concentrations of Na⁺_i. Calcium in the pipette, to be transported, was 8 mM and all currents were activated in the absence of regulatory Ca²⁺_i. Except for the lowest concentration of Na⁺_i examined (10 mM), currents rise rapidly to a peak, followed by a slow decay until steady state levels are attained. The accelerated decay of current with increasing Na⁺_i reflects the Na⁺_i-induced inactivation process (Hilgemann et al., 1992a). Note that the extent of inactivation is greater for CALX1.2 than for CALX1.1. On the other hand, the rate of inactivation of CALX1.1 consistently exceeded that of CALX1.2. For currents activated by 100 mM Na⁺_i, for example, the decay rate constants, λ (see APPENDIX), for CALX1.1 and CALX1.2 were 0.49 ± 0.19 s⁻¹ (mean ± SD, n = 74) and 0.22 ± 0.05 s⁻¹ (mean ± SD, n = 38), respectively. Differences in the current-voltage relationships of the CALX isoforms were not observed (data not shown).

Pooled data from seven Na⁺_i titration experiments for CALX1.1 and CALX1.2 are summarized in Fig. 3. Values for peak and steady state currents were obtained by curve-fitting individual current transients to a single-exponential function (APPENDIX, Eq. A4). Averaged data were normalized to peak (Fig. 3 A) or steady state (Fig. 3 B) currents obtained in response to 100 mM Na⁺_i, followed by curve-fitting to the Hill equation (AP-

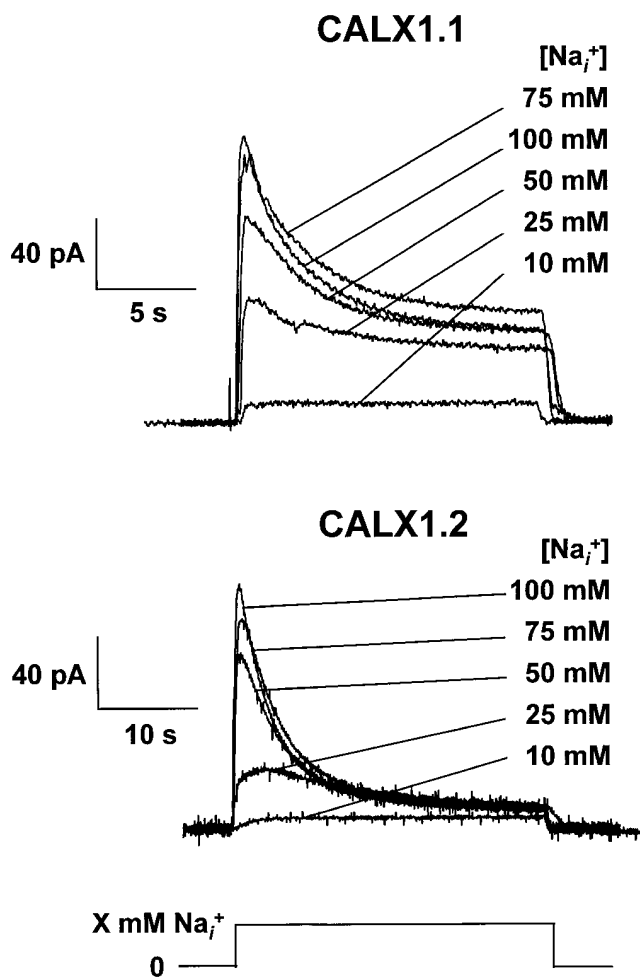


FIGURE 2. The Na^+ dependence of outward $\text{Na}^+\text{-Ca}^{2+}$ exchange currents for CALX isoforms. Overlapping current traces for both CALX isoforms are shown. Outward currents were activated in the absence of regulatory Ca^{2+} , by application of the indicated concentrations of Na^+ , maintained until a steady state was attained, followed by switching back to a Li^+ -based bath solution.

PENDIX, Eq. A7) to determine the Na^+ concentrations producing half-maximal (i.e., K_d values) peak and steady state exchange currents. The apparent values for peak K_d were essentially the same for both exchangers (35.2 ± 2.3 and 34.2 ± 1.1 mM for CALX1.1 and CALX1.2, respectively), whereas the steady state K_d value for CALX1.2 was slightly lower than that of CALX1.1 (16.6 ± 1.0 and 11.6 ± 0.7 mM for CALX1.1 and CALX1.2, respectively).

The most obvious difference between the CALX1.1 and CALX1.2 responses to Na^+ application was the extent to which they underwent I_1 inactivation (Fig. 2). This is quantitated in Fig. 4, where the ratios of steady state to peak exchange currents, F_{ss} , are plotted against Na^+ (see also Fig. 2). The ratio, F_{ss} , serves as a measure of the extent of Na^+ -dependent inactivation (see APPENDIX). For all Na^+ concentrations above 10 mM, the

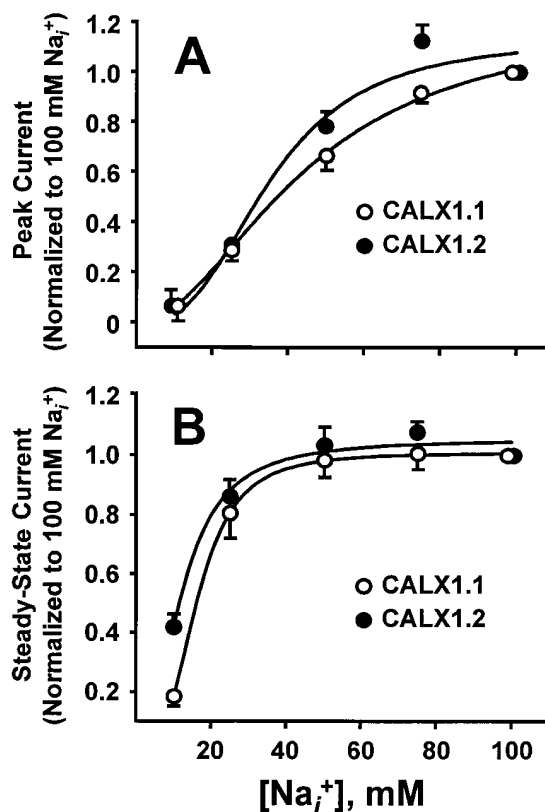


FIGURE 3. The Na^+ dependence of peak and steady state outward $\text{Na}^+\text{-Ca}^{2+}$ exchange currents for CALX isoforms. Data from seven patches for each exchanger were normalized to the peak (A) and steady state (B) currents generated by application of 100 mM Na^+ in the absence of regulatory Ca^{2+} . Data were "best-fit" to the Hill equation by least-squares regression analysis.

extent of inactivation was clearly greater for CALX1.2 than for CALX1.1. For example, for currents obtained in response to 100 mM Na^+ application, F_{ss} values for CALX1.1 and CALX1.2 were 0.26 ± 0.06 (mean \pm SD, $n = 74$) and 0.14 ± 0.04 (mean \pm SD, $n = 38$). In the simplest case, these differences might reflect accelerated entry into, or impeded exit from, the Na^+ -induced inactive state for CALX1.2 as compared with CALX1.1.

To further investigate the differences in Na^+ -induced inactivation between the two CALX isoforms, we performed paired-pulse experiments to determine the rates of recovery from the I_1 inactive state. Typical traces from experiments of this type are shown in Fig. 5 (top three panels). Currents were activated by applying 100 mM Na^+ until a steady state current level was achieved. Intracellular Na^+ was then removed for a variable recovery period (0.5–48 s) before the delivery of a second pulse of 100 mM Na^+ . The magnitude of the second peak reflects the extent to which the exchanger population has recovered from Na^+ -induced inactivation, analogous to paired-pulse experiments for ion channels (Hille et al., 1984; Hilgemann et al.,

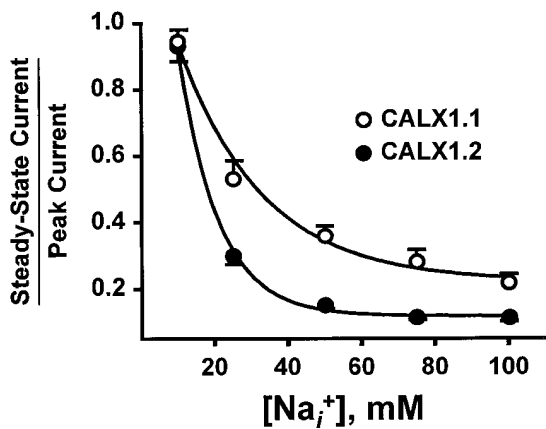


FIGURE 4. The Na_i^+ dependence of F_{ss} , the ratio of steady state to peak currents, for CALX isoforms. The Na_i^+ dependence of the ratio of steady state to peak outward currents for CALX1.1 and CALX1.2 is shown. Values are mean \pm SEM of six to seven determinations for CALX1.1 and four to six determinations for CALX1.2.

1992a). Note that complete recovery is observed at longer intervals (e.g., 48 s), whereas little to no recovery is evident at shorter intervals (e.g., 2 s). Fig. 5 (bottom) summarizes data obtained from 13 patches of CALX1.1 and 5 of CALX1.2 spanning 0.5–48-s recovery intervals. Data were curve-fitted to Eq. A6 (see APPENDIX) and the recovery rate constants, β , were determined as $0.13 \pm 0.01 \text{ s}^{-1}$ and $0.05 \pm 0.01 \text{ s}^{-1}$ for CALX1.1 and CALX1.2, respectively. These results show an approximately threefold reduction in the rate of recovery from I_1 inactivation for CALX1.2 as compared with CALX1.1, indicating greater stability of the I_1 inactive state of CALX1.2. As we have no direct experimental means of obtaining discrete values for α or f_{3m} , we do not report values for entry into the I_1 inactive state. A complete description of the rate constants α , β , and λ , and the analytical approach used, is given in APPENDIX.

Ca_i^{2+} Regulation of Na^+ - Ca^{2+} Exchange Currents

All native Na^+ - Ca^{2+} exchangers examined to date are influenced by regulatory Ca_i^{2+} . So far, the Na^+ - Ca^{2+} exchanger from *Drosophila*, CALX1.1, is unique in exhibiting a negative regulatory influence of cytoplasmic Ca^{2+} (Hryshko et al., 1996). Here, we show that both isoforms of the *Drosophila* Na^+ - Ca^{2+} exchanger exhibit negative regulation by Ca_i^{2+} . However, there are substantial differences in the nature of this inhibition. In Fig. 6, outward currents were activated by applying 100 mM Na_i^+ . After steady state current levels were achieved, 1 μM regulatory Ca_i^{2+} was applied, and then removed. For CALX1.1, the application of regulatory Ca_i^{2+} leads to a substantial inhibition of current that then recovers to steady state levels upon Ca_i^{2+} removal.

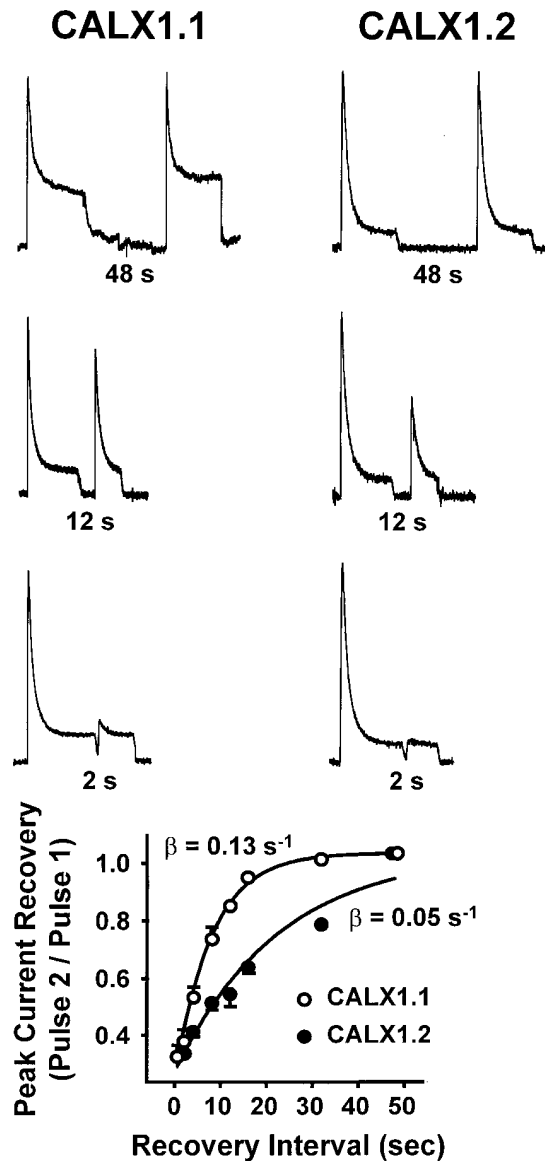


FIGURE 5. The rate of recovery from Na_i^+ -induced inactivation of peak outward Na^+ - Ca^{2+} exchange currents for CALX isoforms. The top three panels show representative current traces obtained from paired-pulse experiments with 48-, 12-, and 2-s recovery intervals. Currents were activated by 100 mM Na_i^+ , in the absence of regulatory Ca_i^{2+} , and maintained until a steady state level was obtained (i.e., Pulse 1). Current was then deactivated by rapidly switching to 100 mM Li_i^+ . After a recovery period of 0.5–48 s, a second pulse of 100 mM Na_i^+ was delivered (i.e., Pulse 2). The bottom summarizes data obtained from 13 patches of CALX1.1 and 5 of CALX1.2 spanning recovery intervals of 0.5–48 s. Data were “best-fit” to a single-exponential function via least-squares regression analysis.

In contrast, regulatory Ca_i^{2+} is nearly without effect on steady state currents from CALX1.2. Nine patches for CALX1.2 were studied using this protocol and we observed small increases or decreases ($\approx 5\%$) or no change in response to the application of 1 μM Ca_i^{2+} . In

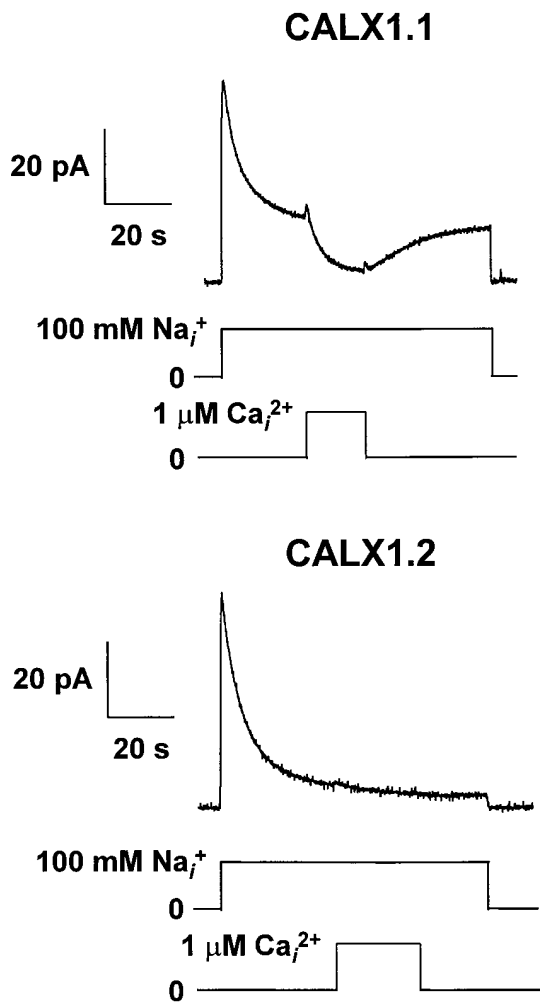


FIGURE 6. The effect of regulatory Ca^{2+}_i on steady state Na^+ - Ca^{2+} exchange currents for CALX isoforms. Representative data are shown illustrating outward currents generated by CALX1.1 and CALX1.2 in response to the application of 100 mM Na^+_i . Regulatory Ca^{2+}_i (1 μM) was applied in the middle of the current record (near steady state), and then removed as indicated. Note that currents are substantially inhibited by regulatory Ca^{2+}_i for CALX1.1 but not for CALX1.2.

contrast, the inhibition observed with CALX1.1 is typical for 41 patches. These traces show striking differences in the response to regulatory Ca^{2+}_i between the two isoforms. Nevertheless, both exchangers are inhibited by regulatory Ca^{2+}_i , as described below.

The influence of regulatory Ca^{2+}_i on peak current generated by CALX1.1 and CALX1.2 is shown in Fig. 7. Currents were activated by the rapid application of 100 mM Na^+_i in the absence or presence of various concentrations of regulatory Ca^{2+}_i . Regulatory Ca^{2+}_i at the indicated concentrations was present before and during current activation, and transported Ca^{2+}_o in the pipette was constant at 8 mM. Note that both exchangers exhibit a decrease in current magnitude in the presence

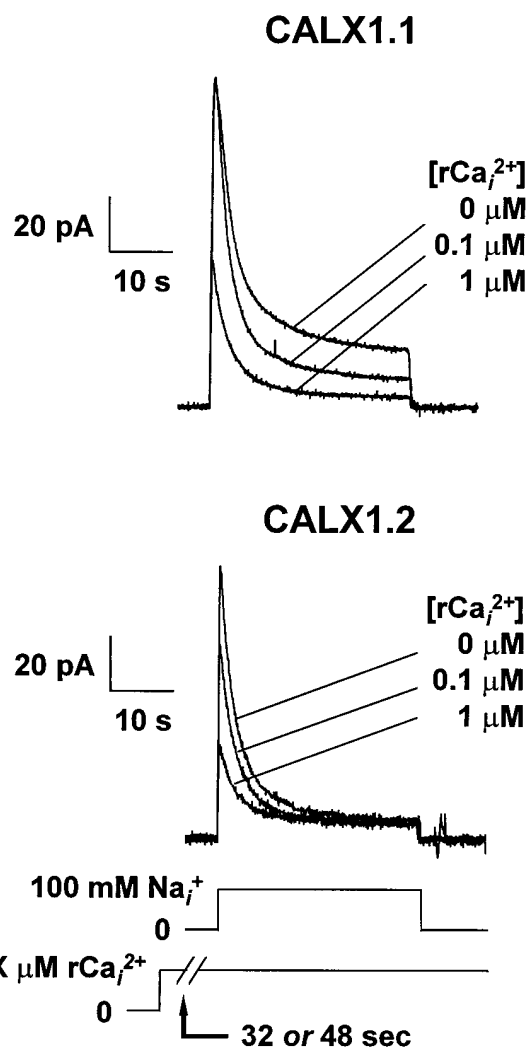


FIGURE 7. The effect of preincubation with regulatory Ca^{2+}_i on Na^+ - Ca^{2+} exchange current transients for CALX isoforms. Representative data are shown for outward Na^+ - Ca^{2+} exchange currents activated by 100 mM Na^+_i . Regulatory Ca^{2+}_i at the indicated concentrations was present before and during current activation.

of regulatory Ca^{2+}_i (i.e., negative Ca^{2+}_i regulation). However, two major differences between these isoforms can be seen from the current traces. First, Ca^{2+}_i exhibits pronounced effects on both peak and steady state currents for CALX1.1, as previously reported (Hryshko et al., 1996). In contrast, the effects of regulatory Ca^{2+}_i are prominent on peak currents but much less pronounced for steady state currents for CALX1.2. Second, though less obvious from these traces, is the observation that regulatory Ca^{2+}_i exerts effects at much lower concentrations for CALX1.2 than for CALX1.1. These relationships are most apparent from the pooled data shown below.

Fig. 8 illustrates results from 10 patches for CALX1.1 and 8 for CALX1.2. Peak and steady state currents were

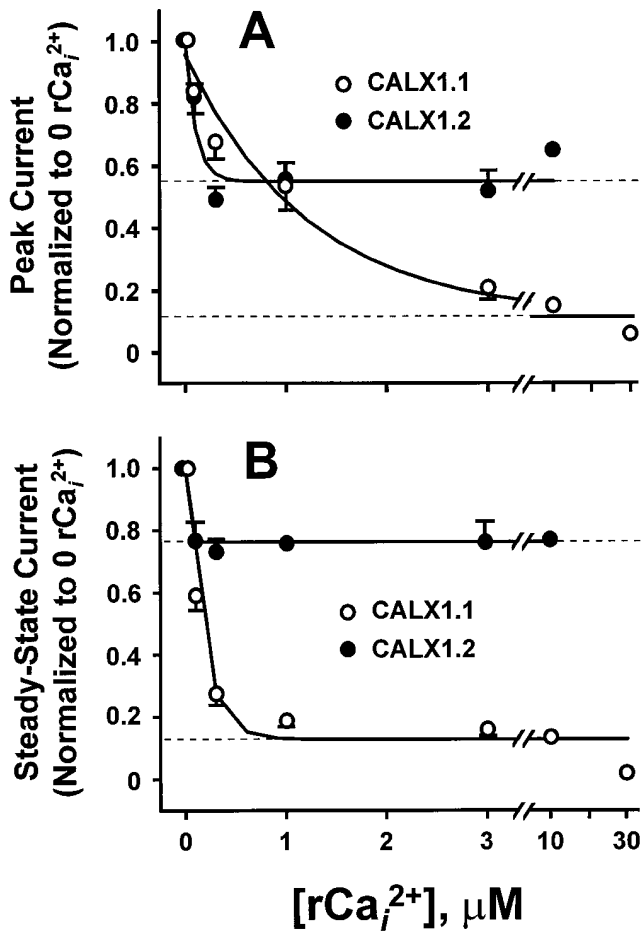


FIGURE 8. The effect of regulatory Ca^{2+}_i on peak and steady state Na^+ - Ca^{2+} exchange currents for CALX isoforms. Peak (A) and steady state (B) currents for CALX1.1 (10 patches) and for CALX1.2 (8 patches) generated in experiments in which giant patches were incubated with the indicated concentrations of regulatory Ca^{2+}_i (rCa_i^{2+}), as in Fig. 7, were normalized to the peak or steady state currents obtained in the absence of rCa_i^{2+} . Values are mean \pm SEM of four to six determinations for CALX1.1 (except at 10 and 30 μM rCa_i^{2+} , which are from one and two determinations, respectively) and four to eight for CALX1.2 (except at 10 μM rCa_i^{2+} , which is from a single determination). Data were “best-fit” to a two-parameter, single-exponential function via least-squares regression analysis. Dotted lines represent the estimated minimum values of peak and steady state currents.

normalized to the values obtained in the absence of regulatory Ca^{2+}_i . Note that for peak currents, the affinity for Ca^{2+}_i regulation is greater for CALX1.2, but the extent of inhibition is considerably less. In contrast, CALX1.1 shows lower affinity but greater efficiency for negative Ca^{2+}_i regulation. For steady state currents, large differences in the extent of negative Ca^{2+}_i regulation are observed between the splice variants. The affinity for negative Ca^{2+}_i regulation is also higher for CALX1.2, with the effect being essentially complete at 300 nM Ca^{2+}_i . This high affinity, low efficiency effect partially

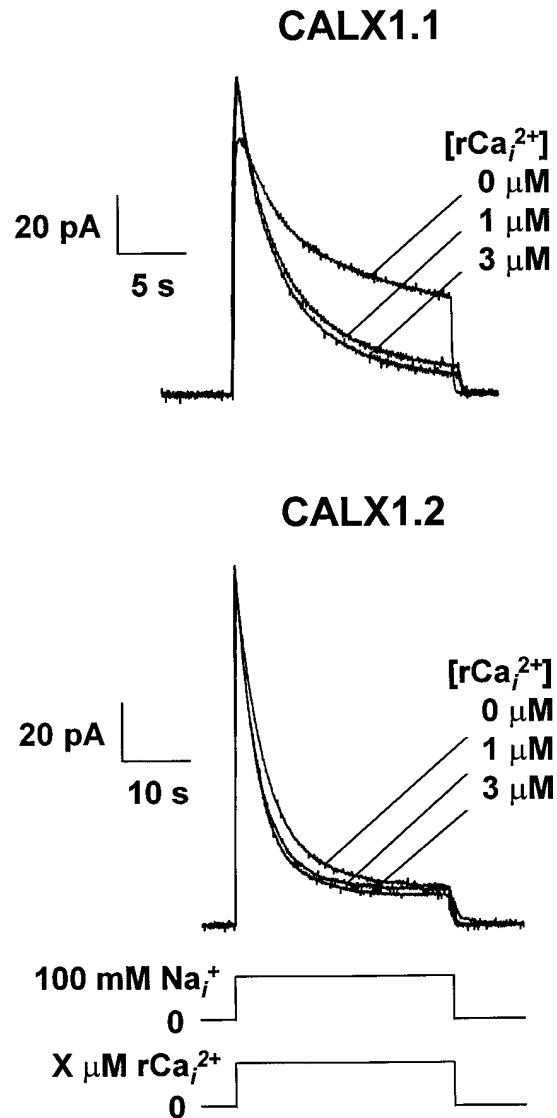


FIGURE 9. The effect of regulatory Ca^{2+}_i on Na^+ - Ca^{2+} exchange current transients for CALX isoforms. Representative data are shown for outward Na^+ - Ca^{2+} exchange currents activated by 100 mM Na^+ . Regulatory Ca^{2+}_i at the indicated concentrations was present during current activation only.

accounts for the minimal influence of regulatory Ca^{2+}_i application shown in Fig. 5 above. In contrast, the lower affinity, higher efficiency effects of regulatory Ca^{2+}_i on CALX1.1 are seen in this graph and Fig. 5.

To gain further insight into these differences, we examined the influence of regulatory Ca^{2+}_i using two additional protocols. First, we examined how regulatory Ca^{2+}_i influenced outward currents if applied at the same time as Na^+ to activate the current. That is, regulatory Ca^{2+}_i was absent before current activation. Under these conditions, the exchanger population should be maximally available as the inhibitory influences of both Na^+ and Ca^{2+}_i are absent before current activa-

tion. For both exchangers, this appeared to be the case, as shown in Fig. 9. Here, both CALX isoforms show similar peak currents, independent of the concentration of regulatory Ca^{2+}_i applied during the pulse. That is, the initial current peak reflects the maximal number of exchangers producing peak current before inhibition by regulatory Ca^{2+}_i . The resultant waveforms then slowly decay to steady state values, appropriate for the concentration of regulatory Ca^{2+}_i present. This indicates that negative regulation by Ca^{2+}_i for *Drosophila* exchangers is a relatively slow process. In contrast, activation of exchange current by regulatory Ca^{2+}_i is extremely rapid (i.e., within solution switch time of ≈ 0.2 s) for the cardiac exchanger, NCX1 (Hilgemann et al., 1992b). Also, the large difference between CALX1.1 and CALX1.2 for the effects of regulatory Ca^{2+}_i on steady state currents is apparent.

The second approach investigated the influence of Ca^{2+}_i in paired-pulse experiments to determine how regulatory Ca^{2+}_i influenced recovery from Na^+ -induced inactivation. Fig. 10 (left) shows paired pulses for 4-s recovery intervals, with or without regulatory Ca^{2+}_i present, for both CALX isoforms. For ease of comparison, currents were normalized to the height of the first peak of each pair. This normalization obscures the inhibitory effects of regulatory Ca^{2+}_i but allows for simple comparison of recovery behavior. All currents were activated by 100 mM Na^+ , and regulatory Ca^{2+}_i was either

absent or present at 300 nM. For CALX1.1, the rate of recovery is clearly decreased when regulatory Ca^{2+}_i is present. This is exactly opposite to that observed for NCX1, where increasing regulatory Ca^{2+}_i accelerates I_1 recovery (Hilgemann et al., 1992b; data not shown). Recovery from Na^+ -induced inactivation for CALX1.2 is increased in the presence of regulatory Ca^{2+}_i . Thus, the behavior of CALX1.2 is directionally similar to that of NCX1 and opposite to that of CALX1.1.

This effect of regulatory Ca^{2+}_i is shown for a range of recovery intervals for the CALX isoforms (Fig. 10, right). The results are from single patches where the complete range of recovery intervals were obtained in the absence and presence of 300 nM regulatory Ca^{2+}_i . Although we could not routinely complete the entire protocol at two Ca^{2+}_i concentrations (which requires that the giant membrane patch remains viable for 30–45 min), we observed this increase in recovery rate for CALX1.2 in five patches and the decrease for CALX1.1 recovery in three patches. Thus, CALX1.2 responds oppositely to CALX1.1 with respect to the influence of Ca^{2+}_i on recovery from I_1 inactivation. This behavior, in conjunction with the diminished I_2 effects (Figs. 7 and 8), provides a reasonable account as to why regulatory Ca^{2+}_i has virtually no effect on CALX1.2 steady state currents (Fig. 6). For CALX1.2, the small decrease in current mediated by negative Ca^{2+}_i regulation is offset by a reduction in Na^+ -induced inactivation.

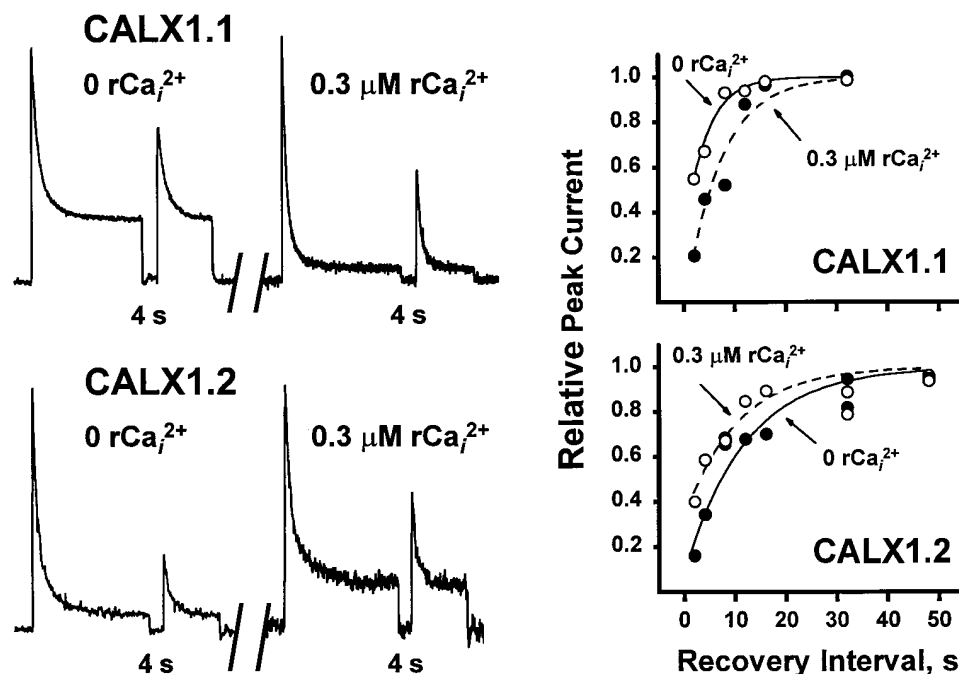


FIGURE 10. The effect of regulatory Ca^{2+}_i on rates of recovery from Na^+ -induced inactivation for CALX isoforms. (left) Outward Na^+ - Ca^{2+} current traces were obtained from a single patch of each isoform in paired-pulse experiments with 4-s recovery intervals (see Fig. 5) in which the effects of 0 and 300 nM regulatory Ca^{2+}_i were assessed. The condition of 0 or 300 nM Ca^{2+}_i was initiated before delivery of the first pulse of 100 mM Na^+ , and maintained throughout activation, recovery, and activation of the second pulse. Currents were normalized to the height of the first, control Na^+ pulse to allow for simple comparison of recovery behavior. (right) Graphs summarize the data from these two patches obtained for the full range of recovery intervals (i.e., 0.5–48 s) in the absence and presence of 300 nM Ca^{2+}_i . Data were normalized to the height of the first peak of each pair and “best-fit” to a single-exponential function (Eq. A6) via least-squares regression analysis.

DISCUSSION

We have shown that two alternatively spliced isoforms of the $\text{Na}^+\text{-Ca}^{2+}$ exchanger from *Drosophila* exhibit substantial differences in ionic regulation by Na^+_i and Ca^{2+}_i . While numerous splice variants have been identified for $\text{Na}^+\text{-Ca}^{2+}$ exchangers using molecular biological techniques, this is the first demonstration of functional differences in ionic regulatory properties between two such isoforms. That ionic regulatory mechanisms have been targeted by nature for modification is suggestive of the importance of these mechanisms in tissue-specific physiological function.

Na⁺_i-induced Inactivation

Sodium-induced inactivation of $\text{Na}^+\text{-Ca}^{2+}$ exchange currents is a process that appears to be analogous to inactivation of ion channels (Hilgemann et al., 1992a). In the simplest case, this inactivation reflects removal of a fraction of the population of exchangers available for transport (see APPENDIX). Evidence supporting altered transport properties for the entire population of exchangers is lacking (Hilgemann et al., 1992a), and recent studies indicate that exchangers partition between fully active and inactive states (Hilgemann, 1996). Consequently, steady state current levels occur when entry into and exit from the inactive state are equal. As described by Hilgemann et al. (1992a), entry into the I_1 inactive state occurs from the 3 Na^+_i -loaded form of the exchanger with transport sites facing the cytoplasmic side. Elevations in cytoplasmic Na^+ augment inactivation by increasing the fraction of exchangers in the 3 Na^+_i -bound configuration. We have used this model of I_1 inactivation to interpret differences in Na^+_i -induced inactivation between the two $\text{Na}^+\text{-Ca}^{2+}$ exchanger isoforms from *Drosophila*.

Compared with CALX1.1, CALX1.2 exhibits substantially greater Na^+_i -dependent inactivation based on all criteria examined. We have used F_{ss} , the ratio of steady state to peak current, as a measure of the extent of steady state inactivation. This value reflects the population of exchangers contributing to steady state current compared with that producing peak current. There is a substantial decrease in steady state current levels for CALX1.2 as compared with CALX1.1. These changes in F_{ss} could reflect either an increased entry rate into, or a decreased recovery rate from, the I_1 inactive state. To discriminate between these possibilities, we conducted paired-pulse experiments. Within the framework of the I_1 inactivation model, these experiments isolate the rate of recovery from inactivation since Na^+_i is absent during recovery periods and, therefore, entry into the I_1 state cannot occur (see APPENDIX). We observed that the rate of recovery from inactivation is decreased nearly threefold for CALX1.2, indicating that

the stability of the I_1 inactive configuration is much greater for CALX1.2 than for CALX1.1. Although the exact mechanism of Na^+_i -induced inactivation remains unknown, a reasonable picture is beginning to emerge based on structure–function studies and electrophysiological analyses. Mutations within the XIP region of NCX1 lead to marked changes in Na^+_i -dependent inactivation that can either accelerate or eliminate I_1 inactivation (Matsuoka et al., 1997). Our initial structure–function studies for CALX1.1 have revealed that analogous mutations produce regulatory phenotypes analogous to those of NCX1 (Dyck et al., 1997). Both NCX1 and CALX1.1 are inhibited by the exogenous application of the peptide inhibitor, XIP (Li et al., 1991; Hryshko et al., 1996). We speculate that exogenous application of XIP inhibits exchange currents by mimicking the inactivation process. By analogy to mechanisms well-described for ion channels, the XIP region may represent an inhibitory domain that plays a prominent role in the transition from active to inactive states of the exchanger. Electrophysiological studies of Na^+_i -dependent inactivation strongly support the notion that inactivation reflects such a transition (Hilgemann et al., 1992b; Hilgemann, 1996). The present data indicate that the alternatively spliced region serves a role in establishing the extent and rapidity of Na^+_i -dependent inactivation, since marked changes in this property are observed between isoforms. It remains to be determined how this region influences Na^+_i -dependent inactivation.

Ca²⁺_i-dependent Regulation

Calcium-dependent regulation of the cardiac exchanger, NCX1, appears as the augmentation of outward exchange currents in response to the application of micromolar levels of cytoplasmic Ca^{2+} (Hilgemann, 1990; Hilgemann et al., 1992b; Matsuoka et al., 1995). Regulatory Ca^{2+}_i affects at least two processes. First, it strongly influences Na^+_i -dependent inactivation. At higher Ca^{2+}_i concentrations (e.g., 10 μM), Na^+_i -dependent inactivation can be eliminated and current traces no longer exhibit decay. Second, regulatory Ca^{2+}_i activates the exchanger population directly. Removal of Ca^{2+}_i favors a slow (i.e., seconds) entry into the I_2 inactive state. Conversely, exit from the I_2 state by addition of regulatory Ca^{2+}_i is extremely rapid and occurs within solution switch times for NCX1.

Structure–function studies (using mutagenesis and electrophysiology experiments) and biochemical studies (using fusion protein and ^{45}Ca -overlay experiments) have identified a protein region comprising the high affinity, regulatory Ca^{2+}_i binding site of NCX1 (Levitsky et al., 1994; Matsuoka et al., 1995). This region encompasses amino acids 371–508 and is modeled to reside near the middle of the large intracellular loop between trans-

membrane segments five and six. Prominent within this region are two well-conserved, highly acidic clusters of amino acids. Mutations within these acidic clusters lead to significant alterations in the affinity for Ca^{2+}_i regulation in both NCX1 and CALX1.1, as assessed by the giant excised patch technique (Matsuoka et al., 1995; Dyck et al., 1997).

The two, alternatively spliced isoforms of the Na^+ - Ca^{2+} exchanger from *Drosophila* are unique among all characterized mammalian exchangers in that they exhibit negative regulation by cytoplasmic Ca^{2+}_i . Alternative splicing does not change the negative regulatory phenotype, although considerable differences are observed in the properties of Ca^{2+}_i regulation. Specifically, CALX1.1 shows considerably greater inhibition by regulatory Ca^{2+}_i , albeit at higher concentrations. While CALX1.2 shows high affinity for Ca^{2+}_i regulation, the extent of inhibition is small. Maximum inhibition for both steady state and peak currents is only $\approx 20\text{--}40\%$ as compared with $>80\%$ for CALX1.1. This difference is most obvious for steady state currents that show only marginal inhibition by Ca^{2+}_i for CALX1.2. These data indicate that alternative splicing influences both Na^+ - and Ca^{2+}_i -dependent regulatory mechanisms.

Interactions between Na^+ - and Ca^{2+}_i -dependent Regulation

The interactions between Na^+ - and Ca^{2+}_i -dependent regulation are best described for the native Na^+ - Ca^{2+} exchanger from measurements of sarcolemmal membrane “blebs” (Hilgemann et al., 1992*b*). However, this interaction is also evident using the *Xenopus* oocyte expression system and the cloned cardiac exchanger, NCX1 (Matsuoka et al., 1995; Trac et al., 1996). In both assay systems, it was observed that regulatory Ca^{2+}_i could completely eliminate Na^+ -dependent inactivation and that the extent of Na^+ -dependent inactivation was graded progressively by regulatory Ca^{2+}_i levels. From extensive modeling, it appears that regulatory Ca^{2+}_i accelerates exit from and reduces entry into the I_1 inactive state for NCX1 (Hilgemann et al., 1992*b*). Structurally, it remains unknown how this interaction occurs. In this study, we examined the interaction between Na^+ -dependent inactivation and regulatory Ca^{2+}_i using Ca^{2+}_i preincubation and paired-pulse experiments. Surprisingly, we observed exactly opposite results for CALX1.1 than those reported for NCX1. That is, Ca^{2+}_i stabilized the I_1 inactive state of CALX1.1. Also, both CALX isoforms react to Ca^{2+}_i application slowly (over seconds), whereas NCX1 responds within solution switch times. Furthermore, Na^+ -dependent inactivation for CALX1.2 was alleviated by the addition of regulatory Ca^{2+}_i , similar to NCX1 and opposite to CALX1.1. These striking differences between exchangers may prove important towards understanding the transduction of the regulatory Ca^{2+} binding signal.

Significance

Our results indicate that Na^+ - and Ca^{2+}_i -dependent regulatory mechanisms are altered in the alternatively spliced Na^+ - Ca^{2+} exchanger isoforms from *Drosophila*. This is the first demonstration of alterations in regulatory mechanisms for splice variants of Na^+ - Ca^{2+} exchangers. Our data suggest that alternative splicing may provide an efficient means of modifying behavior, possibly to fulfill specific tissue requirements. That alternative splicing alters regulatory properties implies that these mechanisms may be important in the physiological function of the multi-gene family of Na^+ - Ca^{2+} exchangers. We have also identified differences in ionic regulation between tissue-specific, alternatively spliced mammalian exchangers from kidney, heart, and brain (Hnatowich, M., C. Dyck, A. Omelchenko, B. Quednau, K.D. Philipson, and L.V. Hryshko, manuscript in preparation). These data provide increasing support for the possibility that ionic regulation fulfills a role in physiological Na^+ - Ca^{2+} exchange function. Alternative splicing may contribute to this role.

APPENDIX

Following the two-step Na^+ -dependent inactivation model proposed by Hilgemann et al. (1992*a*, 1992*b*), we consider that entry into the I_1 inactive state is related to the fraction of exchangers loaded with 3 Na^+ , termed $f_{3\text{ni}}$, and recovery from I_1 inactivation is a simple, time-dependent (i.e., first-order) process. The fraction, χ , of the entire exchanger population being in an active state is given by the equation:

$$\frac{d\chi}{dt} = \beta(1 - \chi) - \alpha f_{3\text{ni}}\chi, \quad (\text{A1})$$

where α is an inactivation rate constant and β is a recovery (from I_1 inactivation) rate constant. For CALX isoforms, the maximal population of active exchangers, χ_∞ , is assumed to be available only in the absence of regulatory Ca^{2+}_i and before Na^+ application. Under these conditions, entry into Na^+ - and Ca^{2+}_i -dependent inactive states cannot occur. Thus, with CALX isoforms, it is possible to study Na^+ -dependent inactivation in the absence of modulating influences by regulatory Ca^{2+}_i . The solution to Eq. A1 is:

$$\chi_t = \chi_\infty + (1 - \chi_\infty) e^{-\lambda t}, \quad (\text{A2})$$

where $\lambda = \alpha f_{3\text{ni}} + \beta$, is a current decay rate constant, and $\chi_\infty = \beta/\lambda$, is the steady state fraction of active exchangers.

Since the rate of inactivation is much slower (i.e., seconds) than the transport rate and the rate at which the Na^+ concentration can be altered (i.e., ≈ 0.2 s; Collins et al., 1992), all current transients will reflect the time-

dependent process of inactivation and recovery. Therefore, the expressions for the peak, I_{peak} , and steady state currents, I_{ss} , are given by:

$$I_{\text{peak}} = \chi_o Ni \quad I_{\text{ss}} = \chi_\infty Ni, \quad (\text{A3})$$

where N is the number of exchangers and i is the elementary current of the fully active individual $\text{Na}^+\text{-Ca}^{2+}$ exchanger. An expression for the time dependence of outward exchange current, reflecting Na^+ -dependent changes in the population of active exchangers, is obtained by combining Eqs. A2 and A3 to give:

$$I_t = I_{\text{peak}} \left[\frac{\beta}{\lambda} + \left(1 - \frac{\beta}{\lambda} \right) e^{-\lambda t} \right]. \quad (\text{A4})$$

This equation was used for fitting current transients obtained from single-pulse experiments.

The ratio of steady state current to the initial peak current, F_{ss} , can serve as a measure of exchange current inactivation. The smaller the value of F_{ss} , the greater the extent of inactivation. In terms of the current decay rate constant, λ , and the recovery from inactivation rate constant, β , we can write (from Eqs. A2 and A3):

$$F_{\text{ss}} = \frac{\beta}{\lambda}. \quad (\text{A5})$$

The transition between inactive and active exchanger states occurring during the recovery period of paired-pulse experiments can be also described by Eq. A1,

with the only difference being that entry into the I_1 inactive state cannot occur since $f_{\text{3ni}} = 0$ at $[\text{Na}^+]_i = 0$. Therefore, the dependence of peak current during the second pulse, $I_{\text{peak}}^{\text{R}}$ on the recovery interval, t_{R} , reads:

$$I_{\text{peak}}^{\text{R}} = I_{\text{peak}} \left[1 - \left(1 - \frac{\beta}{\lambda} \right) e^{-\beta t_{\text{R}}} \right]. \quad (\text{A6})$$

Here I_{peak} corresponds to the peak current during the first Na^+ application (i.e., after full recovery from I_1 inactivation after ≈ 48 s). It can be seen from Eq. A6 that paired-pulse experiments reveal the rate constant of recovery, β , alone, while the current decay rate, λ , obtained from single-pulse experiments, represents the sum of both inactivation, α , and recovery, β , rate constants.

Half-saturating Na^+ concentrations, K_d , indicative of the apparent Na^+ affinities of $\text{Na}^+\text{-Ca}^{2+}$ exchange for peak and steady state currents (both designated in Eq. A7 as I), were obtained by fitting the Na^+ dependence of the corresponding currents to the Hill equation, as follows:

$$I = \frac{I_{\text{max}} [\text{Na}_i]^X}{[\text{Na}_i]^X + K_d^X}, \quad (\text{A7})$$

where $[\text{Na}_i]$ is the Na^+ concentration, I_{max} is the fitted peak or steady state exchange current at $[\text{Na}_i] \rightarrow \infty$, and X is the Hill coefficient.

This work was supported by grants from the Medical Research Council of Canada, the Manitoba Health Research Council, and the Heart and Stroke Foundation of Canada (to L.V. Hryshko) and by National Institutes of Health grants HL-48509 and HL-49101 (to K.D. Philipson and D.A. Nicoll). C. Dyck is supported by a studentship from the Manitoba Health Research Council and L.V. Hryshko by a scholarship from the Medical Research Council of Canada.

Original version received 4 February 1998 and accepted version received 18 March 1998.

REFERENCES

- Barnes, K.V., G. Cheng, M.M. Dawson, and D.R. Menick. 1997. Cloning of cardiac, kidney, and brain promoters of the feline *ncx1* gene. *J. Biol. Chem.* 272:11510–11517.
- Bers, D.M. 1991. Excitation–Contraction Coupling and Cardiac Contractile Force. Kluwer Academic Publications, London, UK. 71–92.
- Bers, D.M., C.W. Patton, and R. Nuccitelli. 1994. A practical guide to the preparation of Ca^{2+} buffers. *Methods Cell Biol.* 40:3–29.
- Blaustein, M.P., G. Fontana, and R.S. Rogowski. 1996. The $\text{Na}^+\text{-Ca}^{2+}$ exchanger in rat brain synaptosomes: kinetics and regulation. *Ann. NY Acad. Sci.* 779:300–317.
- Collins, A., A. Somlyo, and D.W. Hilgemann. 1992. The giant cardiac membrane patch method: stimulation of outward Na/Ca exchange current by MgATP . *J. Physiol. (Camb.)* 454:37–57.
- Dyck, C., J. Buchko, M. Hnatowich, M. Trac, and L.V. Hryshko. 1997. Structure-function studies of Calx, the $\text{Na}^+\text{-Ca}^{2+}$ exchanger from *Drosophila*, reveal conservation of regulatory sites. *Biophys. J.* 72:63a. (Abstr.)
- Hilgemann, D.W. 1990. Regulation and deregulation of cardiac $\text{Na}^+\text{-Ca}^{2+}$ exchange in giant excised sarcolemmal membrane patches. *Nature.* 344:242–245.
- Hilgemann, D.W. 1996. Unitary cardiac Na^+ , Ca^{2+} exchange current magnitudes determined from channel-like noise and charge movements of ion transport. *Biophys. J.* 71:759–768.
- Hilgemann, D.W., S. Matsuoka, G.A. Nagel, and A. Collins. 1992a. Steady-state and dynamic properties of cardiac sodium-calcium exchange: sodium-dependent inactivation. *J. Gen. Physiol.* 100: 905–932.
- Hilgemann, D.W., A. Collins, and S. Matsuoka. 1992b. Steady-state and dynamic properties of cardiac sodium-calcium exchange: secondary modulation by cytoplasmic calcium and ATP. *J. Gen. Physiol.* 100:933–961.
- Hille, B. 1984. Ionic Channels of Excitable Membranes. Sinauer Associates Inc. Sunderland, MA.
- Hryshko, L.V., S. Matsuoka, D.A. Nicoll, J.N. Weiss, E.M. Schwarz, S. Benzer, and K.D. Philipson. 1996. Anomalous regulation of the *Drosophila* $\text{Na}^+\text{-Ca}^{2+}$ exchanger by Ca^{2+} . *J. Gen. Physiol.* 108: 67–74.
- Hryshko, L.V., and K.D. Philipson. 1997. $\text{Na}^+\text{-Ca}^{2+}$ exchange: recent advances. *Basic Res. Cardiol.* 92:45–51.

- Kofuji, P., W.J. Lederer, and D.H. Schulze. 1994. Mutually exclusive and cassette exons underlie alternatively spliced isoforms of the Na/Ca exchanger. *J. Biol. Chem.* 269:5145–5149.
- Leblanc, N., and J.R. Hume. 1990. Sodium current-induced release of calcium from cardiac sarcoplasmic reticulum. *Science.* 248:372–376.
- Lederer, W.J., S. He, S. Luo, W. DuBell, P. Kofuji, R. Kieval, C.F. Neubauer, A. Ruknudin, H. Cheng, M.B. Cannel, T.B. Rogers, and D.H. Schulze. The molecular biology of the Na⁺-Ca²⁺ exchanger and its functional roles in heart, smooth muscle cells, neurons, glia, lymphocytes, and nonexcitable cells. 1996. *Ann. NY Acad. Sci.* 779:7–17.
- Lee, S.L., A.S.L. Yu, and J. Lytton. 1994. Tissue-specific expression of Na⁺-Ca²⁺ exchanger isoforms. *J. Biol. Chem.* 269:14849–14852.
- Levi, A.J., K.W. Spitzer, O. Kohmoto, and J.H.B. Bridge. 1994. Depolarization-induced Ca entry via Na-Ca exchange triggers SR release in guinea pig cardiac myocytes. *Am. J. Physiol.* 266:H1422–H1433.
- Levitsky, D.O., D.A. Nicoll, and K.D. Philipson. 1994. Identification of the high affinity Ca²⁺-binding domain of the cardiac Na⁺-Ca²⁺ exchanger. *J. Biol. Chem.* 269:22847–22852.
- Li, Z., D.A. Nicoll, A. Collins, D.W. Hilgemann, A.G. Filoteo, J.T. Penniston, J.N. Weiss, J.M. Tomich, and K.D. Philipson. 1991. Identification of a peptide inhibitor of the cardiac sarcolemmal Na⁺-Ca²⁺ exchanger. *J. Biol. Chem.* 266:1014–1020.
- Matsuoka, S., D.A. Nicoll, Z. He, and K.D. Philipson. 1997. Regulation of the cardiac Na⁺-Ca²⁺ exchanger by the endogenous XIP region. *J. Gen. Physiol.* 109:1–14.
- Matsuoka, S., D.A. Nicoll, L.V. Hryshko, D.O. Levitsky, J.N. Weiss, and K.D. Philipson. 1995. Regulation of the cardiac Na⁺-Ca²⁺ exchanger by Ca²⁺: mutational analysis of the Ca²⁺ binding domain. *J. Gen. Physiol.* 105:403–420.
- Matsuoka, S., D.A. Nicoll, R.F. Reilly, D.W. Hilgemann, and K.D. Philipson. 1993. Initial localization of regulatory regions of the cardiac sarcolemmal Na⁺-Ca²⁺ exchanger. *Proc. Natl. Acad. Sci. USA.* 90:3870–3874.
- Nicoll, D.A., S. Longoni, and K.D. Philipson. 1990. Molecular cloning and functional expression of the cardiac sarcolemmal Na⁺-Ca²⁺ exchanger. *Science.* 250:561–565.
- Philipson, K.D., D.A. Nicoll, S. Matsuoka, L.V. Hryshko, D.O. Levitsky, and J.N. Weiss. 1996. Molecular regulation of the Na⁺-Ca²⁺ exchanger. *Ann. NY Acad. Sci.* 779:20–28.
- Quednau, B.D., D.A. Nicoll, and K.D. Philipson. 1997. Tissue specificity and alternative splicing of the Na⁺/Ca²⁺ exchanger isoforms NCX1, NCX2, and NCX3 in rat. *Am. J. Physiol.* 272:C1250–C1261.
- Ruknudin, A., C. Valdivia, P. Kofuji, W.J. Lederer, and D.H. Schulze. 1997. Na⁺/Ca²⁺ exchanger in *Drosophila*: cloning, expression, and transport differences. *Am. J. Physiol.* 273:C257–C265.
- Schwarz, E.M., and S. Benzer. 1997. Calx, a Na-Ca exchanger gene of *Drosophila melanogaster*. *Proc. Natl. Acad. Sci. USA.* 94:10249–10254.
- Trac, M., C. Dyck, M. Hnatowich, A. Omelchenko, and L.V. Hryshko. 1997. Transport and regulation of the cardiac Na⁺-Ca²⁺ exchanger: comparison between Ca²⁺ and Ba²⁺. *J. Gen. Physiol.* 109:361–369.